A detailed study on accuracy of uncooled thermal cameras by exploring the data collection workflow

Conference Paper · May 2018

DOI: 10.1117/12.2305217

5 authors, including:

Haoyu Niu
University of California, Merced

Tiebiao Zhao
University of California, Merced

Andreas Anderson
University of California, Merced

YangQuan Chen
University of California, Merced

A detailed study on accuracy of uncooled thermal cameras by exploring the data collection workflow

Tiebiao Zhao, Haoyu Niu, Andreas Anderson, YangQuan Chen, Joshua Viers

Tiebiao Zhao, Haoyu Niu, Andreas Anderson, YangQuan Chen, Joshua Viers, "A detailed study on accuracy of uncooled thermal cameras by exploring the data collection workflow," Proc. SPIE 10664, Autonomous Air and Ground Sensing Systems for Agricultural Optimization and Phenotyping III, 106640F (21 May 2018); doi: 10.1117/12.2305217

SPIE.

Event: SPIE Commercial + Scientific Sensing and Imaging, 2018, Orlando, Florida, United States

A Detailed Study on Accuracy of Uncooled Thermal Cameras by Exploring the Data Collection Workflow

Tiebiao Zhao[a], Haoyu Niu[a], Andreas Anderson[a], YangQuan Chen[a], and Joshua Viers[a]

[a]School of Engineering, University of California, Merced, 5200 North Lake Road, Merced, CA 95343, USA

ABSTRACT

Thermal cameras have been widely used in small Unmanned Aerial Systems (sUAS) recently. In order to analyze a particular object, they can translate thermal energy into visible images and temperatures. The thermal imaging has a great potential in agricultural applications. It can be used for estimating the soil water status, scheduling irrigation, estimating almond trees yields, estimating water stress, evaluating maturity of crops. Their ability to measure the temperature is great, though, there are still some concerns about uncooled thermal cameras. Unstable outdoor environmental factors can cause serious measurement drift during flight missions. Post-processing like mosaicking might further lead to measurement errors. To answer these two fundamental questions, it finished three experiments to research the best practice for thermal images collection. In this paper, the thermal camera models being used are ICI 9640 P-Series, which are commonly used in many study areas. Apogee MI-220 is used as the ground truth. In the first experiment, it tries to figure out how long the thermal camera needs to warm up to be at (or close to) thermal equilibrium in order to produce accurate data. Second, different view angles were set up for thermal camera to figure out if the view angle has any effect on a thermal camera. Third, it attempts to find out that, after the thermal images are processed by Agisoft PhotoScan, if the stitching has any effect on the temperature data.

Keywords: Thermal camera, small Unmanned Aerial System, calibration, mosaicking, stitching

1. INTRODUCTION

Because the uncooled thermal camera is light,[1] low power consumption[2] and less expensive than cooled thermal cameras, it has been widely used in many agricultural applications, such as plant disease detection,[3] crop water stress estimation[4,5] , soil moisture detection[6] and almond trees yields[7,8,9] . Mounted on the Unmanned Aerial Vehicles(UAVs), the uncooled thermal camera make it possible for UAVs to collect high-resolution thermal images in Precision Agriculture(PA).[9] Compared with traditional remote sensing method, such as satellites, the thermal camera and UAVs make the data collection more flexible and lower cost. The cooled thermal cameras are usually more sensitive and accurate than uncooled thermal cameras.[10] But cooled thermal cameras are very big, expensive and energy consuming.[11] So, they can hardly be used on UAVs platform. In contrast, the uncooled thermal camera plays a more and more important role in remote sensing by UAVs platforms.

The thermal camera has so many advantages, though, its micobolometer is not always sensitive and accurate.[11] Also, most thermal cameras are not always calibrated, which makes it can only measure the relative temperature instead of the accurate value. In precision agriculture, however, most time it's necessary to measure the accurate temperature in many applications[1] such as crop monitoring,[12] pest detection[13] and disease detection.[3] We are using thermal camera more and more frequently without understanding it's truth. Therefore, there is a highly strong demand to find a calibration method for the thermal camera in UAVs applications.

Further author information: (Send correspondence to Prof. YangQuan Chen)
Tiebiao Zhao: E-mail: tzhao3@ucmerced.edu
Haoyu Niu: E-mail: hniu2@ucmerced.edu
Andreas Anderson: E-mail: aanderson29@ucmerced.edu
YangQuan Chen: E-mail: ychen53@ucmerced.edu
Joshua Viers: Email jviers@ucmerced.edu

Autonomous Air and Ground Sensing Systems for Agricultural Optimization and Phenotyping III, edited by J. Alex Thomasson, Mac McKee, Robert J. Moorhead, Proc. of SPIE Vol. 10664, 106640F
© 2018 SPIE · CCC code: 0277-786X/18/$18 · doi: 10.1117/12.2305217

Figure 1. Field for thermal camera experiments

Researchers have published many thermal camera calibration methods when they are used in UAVs platforms.[14] In Ref. 11, the author proposed a new calibration algorithm based on neural network.[15] It also improved the photogrammetry process by using Wallis Filter.[16] They increased the measurement accuracy from 3.55 °C to 1.37 °C. In Ref. 1, it implements an internal calibration for a thermal camera controlled by PC 104 embedded computer.[17] The author built a grid with resistive wires. When the wires are heated up, the thermal camera can detect the grid and calibrate the camera. In Ref. 18, the author designed a lab calibration by using a calibration blackbody source(RAYBB400, Raytek, CA,USA). As mentioned above, researchers tried to solve the thermal camera calibration issues, though, the methods used in these papers are not quite appropriate in UAVs platform.[9] For example, the thermal camera can have internal and external disturbance during the drone's flight. Internal disturbance can be caused by microbolometer.[19] For external disturbance, the wind can cool down the thermal cameras. The unstable outdoor environment can also cause serious measurement drift during flight missions. Not all of these factors are considered into the previous papers.

Therefore, in this paper, it mainly focused on the thermal camera calibration in UAVs applications. A thermal cameras needs to be at (or close to) thermal equilibrium in order to produce accurate data. When the camera is turned on, the electronics inside produce heat, and it takes a while for the camera body to heat up enough for the rate of heat loss at the surface to match the rate of heat being produced on the inside. In this paper, it investigates how long the thermal camera should warm up when used in UAVs platforms. Also, when the UAVs are flying in the field, the thermal camera will capture images in different view of angles. In this paper, we also studied the effects of the thermal camera's view of angles on the temperature data we got. For the photogrammetry process, the software Agisoft PhotoScan is frequently used. Thermal images are stitched together into an orthomosaick picture. In this paper, we also figured out if the stitching has any effect on the data process. To our best knowledge, there are no studies talking about these thermal camera calibration issues before.

The paper is organized as follows. In section 2, materials, measurement equipments and methods used in the experiments are mentioned. It includes the thermal camera model, groudntruth model and their functions. In section 3, it discussed how to set up all experiments and all the data is shown in tables and figures. The data was analyzed and several conclusions were reached. In section 4, the paper's work is evaluated and future work is mentioned.

2. MATERIALS AND METHODS

2.1 Study site

This research was conducted in a field near MESA Lab in Atwater, California, USA ($37°22'30.6"N, 120°34'40.9"W$). There were five different materials being used, water, dry soil, wet soil, leaves and white panels. All materials

(a) Experiment field (b) Thermal picture by IR Flash

Figure 2. Calibration's effect experiment

were put in cups, as shown in Figure 1.

2.2 Images collection

The thermal camera ICI 9640 P-Series (ICI, USA) was used to collect thermal images. The thermal camera has a resolution of 640 × 480 pixels. The spectral band is from 7μm to 14 μm. The dimensions of the thermal camera is 34mm × 30mm × 34mm. The accuracy is supposed to be +/- 1°C. In these research experiments, the TIF images were taken for further image processing by Agisoft PhotoScan. The camera was attached under the experiment platform, as shown in Figure 2 (a). The camera was triggered 10 times per second by the ICI Software's function Capture Series Images in ground station computer.

2.3 Groundtruth data collection

The infrared radiometer Apogee MI-220 (Apogee Instruments, Inc) was used in the research experiments to collect thermal data as groundtruth value. The MI-220 has a 18° half-angle field of view (FOV). The response time for the MI-220 is only 0.6 seconds. It can be used in many areas, such as tree canopy temperature measurement,[8] water stress estimation,[20] soil temperature measurement and so on.

3. RESULTS AND DISCUSSIONS

3.1 Experiment Setup

There are three different experiments in this paper. In the first experiment,we analyzed how long it takes for a thermal camera to warm up. Second, we studied the thermal camera's angle effect on the temperature data. Third, we analyzed stiching's effect on the orthomosaick pictures. We prepared five different materials for all experiments to stimulate the situations we might meet in the field. As shown in Figure 2 (b), there are water, wet soil, leaves, dry soil and white paper panels. So, we can analyze the thermal camera's effect on different materials.

3.2 Thermal camera warmup time

A thermal camera needs to be at (or close to) thermal equilibrium in order to produce accurate data. When the camera is turned on, the electronics inside produce heat, and it takes a while for the camera body to heat up enough for the rate of heat loss at the surface to match the rate of heat being produced on the inside.

This poses a challenge to flying a thermal camera on a drone: even if the camera has been given sufficient time to reach equilibrium on the ground, the airflow increases heat transport away from the camera, upsetting the equilibrium again, and requiring additional time to adjust. However, due to the limited flight time of drones, especially multirotors, this time may be longer than the available flight time itself - the recommended equalization time for the camera used in our experiments (an ICI 9640) is about half an hour.

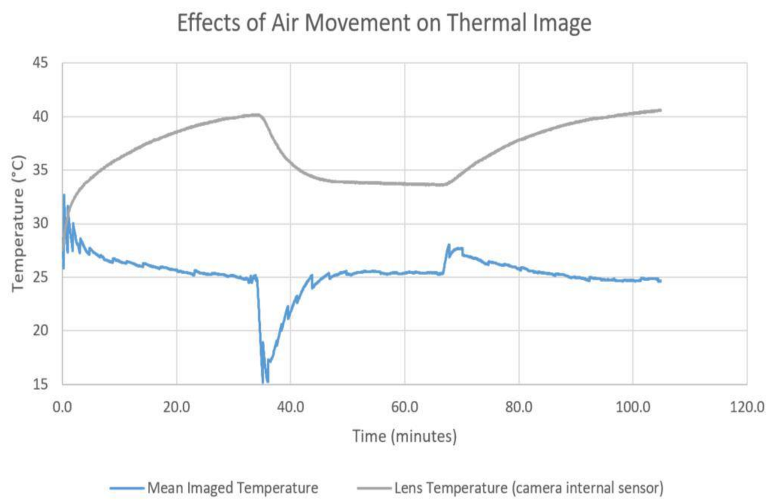

Figure 3. Thermal camera warmup

Our first attempts of mitigation by packing the camera in foam had little success. According to a call to the manufacturer, this was due to the lens being exposed to the airstream, the lens itself being made of a material with high thermal conductivity.

A series of experiments imaging a foam block were conducted. The foam was to provide a uniform surface at room temperature, while the camera was alternately exposed to still air, and air blown from a fan. The average recorded temperature of the image was juxtaposed with the temperature of the lens acquired from the image metadata.

According to Figure 3, the data shows that actively cooling the camera with ambient air can significantly shorten the time until the camera reaches equilibrium. Furthermore, changing the output of the fan after equilibrium was reached has little effect on the measured temperature of the foam block. In Figure 3, average capture rate is 30 frames per minute. At 35 minutes, the fan turned to full power, blowing at lens at a distance of 30cm. At 67 minutes, fan turned off. The sawtooth-like jumps in recorded mean temperature are due to the camera performing non-uniformity corrections (internal calibrations), as it warms up.

3.3 Thermal camera's view angle

In this experiment, the thermal cameras' view angle effect on temperature was tested. In an unmanned aerial vehicle system (UAVs). The thermal cameras are usually mounted on the drones and capturing images when the drones are flying over fields. For example, in an almond trees orchard, the trees canopies can show up in different positions in thermal images. This may cause the canopy has different temperature in different view of angles. In this section, it figured out if the view angles have any effects on the thermal images. The thermal picture has a pixel value of 640×480. The central point pixel value is 320×240. After the test point temperature was got, it also finds the pixel value of the test point. In the thermal picture 1 pixel value represents 0.09525cm. Then one can calculate the horizontal distance between the camera center and the test point. As mentioned in the previous section, the camera's vertical distance to the test point is 69.5325 cm. Then the accurate half view angle can be calculated in this experiment.

According to Table 1, there are 8 different half view angles, 4.2°, 4.6°, 6.0°, 8.3°, 11.6 °, 12.7°, 14.3 °, and 16.7 °. The errors between the groundtruth and the collection data are less than 0.5 °C. The root mean square error is much less than 0.01 °C. The result shows that the the thermal camera's view angles have little effect on collecting data.

Table 1. View angle experiment

Half view angle(°)	Location in the picture	Point temperature(°C)	Groundtruth(°C)
4.2	363 × 275	12.41	12.40
4.6	372 × 269	12.52	12.40
6	354 × 311	11.79	12.40
8.3	352 × 344	12.28	12.40
11.6	342 × 391	12.38	12.40
12.7	337 × 406	12.11	12.40
14.3	336 × 428	11.90	12.40
16.7	329 × 462	12.26	12.40

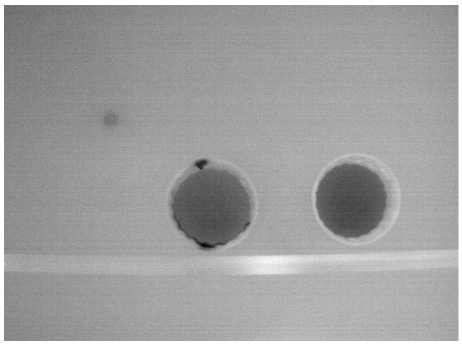

(a) Experiment field

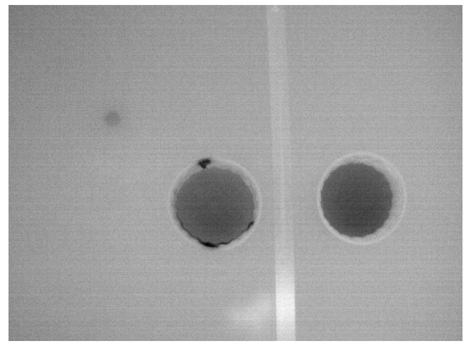

(b) Thermal picture by IR Flash

Figure 4. View angles' effect experiment

3.4 Stiching's effect

After collecting the thermal images, many researchers like to process the data by Agisoft PhotoScan software. In this software, we can stitch all the pictures into one orthomosaick picture which represents the whole field, as shown in Figure 5(b). In this experiment, it figures out if this Align Photos function has any effect on temperature data. As shown in Table 2, there are 28 samples in this experiment. They are divided into four groups, which are water, dry soil, wet soil and white paper panels.There are labels in each picture, so we can accurately find the same temperature point in the single image and the orthomosaick picture.To calculate the temperature, it used the MATLAB 2017b to get the average temperature for a selected area.

Based on Table 2, the temperature errors between the single image and the orthomosaick are less than 1 °C. According to Table 3, for different materials, the root mean square errors are different. For example, the water in a single image has a root mean square error as 0.646 °C. In the orthomosaick picture, the value is 0.834 °C. The result shows the Agisoft PhotoScan's stiching process has a little effect on the thermal data.

4. CONCLUSIONS

In this paper, it discussed three factors' effect on thermal camera calibration. They are fundamental and useful. To our best knowledge, there are no studies talking about these thermal camera calibration issues before. First, the recommended equalization time for the camera used in our experiments (an ICI9640) is about half an hour, it can be an reasonable warmup time for thermal cameras. Second, the thermal camera's view angles have little effect on the temperature data. The thermal camera's accuracy is +/- 1 °C. The data errors in this paper is less than 1 °C and the root mean square error is less than 0.01 °C. Third, after the photogrammetry process, the stitching does have a little effect on the orthomosaick picture we got. The temperature in the orthomosaick is greater than the temperature in single image. This can be caused by the stitching process.

In the future, we will keep working on the thermal camera calibration problem. A more accurate, real time and state-of-art thermal camera calibration method will be proposed in the next paper.

Table 2. Stiching's effect data

Sample number	Materials	Groundtruth(°C)	single image (°C)	orthomosaick(°C)
1	water	17.4	17.74	18.2648
2	water	17.5	17.53	17.9962
3	water	17.4	17.75	18.1876
4	water	17.2	18.23	18.4245
5	water	17.2	16.35	16.5322
6	water	17.4	16.73	17.2438
7	water	16.8	17.47	17.9345
8	dry soil	15.8	15.72	16.6309
9	dry soil	14.4	13.93	14.5372
10	dry soil	14.2	13.53	13.3192
11	dry soil	14.7	14.61	14.8676
12	dry soil	15.4	15.45	15.6241
13	dry soil	14.8	15.51	15.6242
14	dry soil	14.5	15.26	15.3906
15	wet soil	14.8	14.84	15.8454
16	wet soil	13.9	14.38	15.7918
17	wet soil	14.8	14.06	14.9511
18	wet soil	14.1	15.37	14.3389
19	wet soil	14.9	14.89	15.7558
20	wet soil	14.6	14.24	14.8981
21	wet soil	14.3	14.77	15.2562
22	paper	13.6	12.67	13.9083
23	paper	13.8	12.42	12.9427
24	paper	14.5	14.02	15.2562
25	paper	12.8	11.55	13.9083
26	paper	12.4	11.75	12.9427
27	paper	13.9	11.13	12.1386
28	paper	12.4	11.36	11.8678

Table 3. Root mean square error

Materials	Single images(°C)	Orthomosaick(°C)
Water	0.646	0.834
Dry soil	0.503	0.658
Wet soil	0.626	0.963
White panel	0.912	0.949

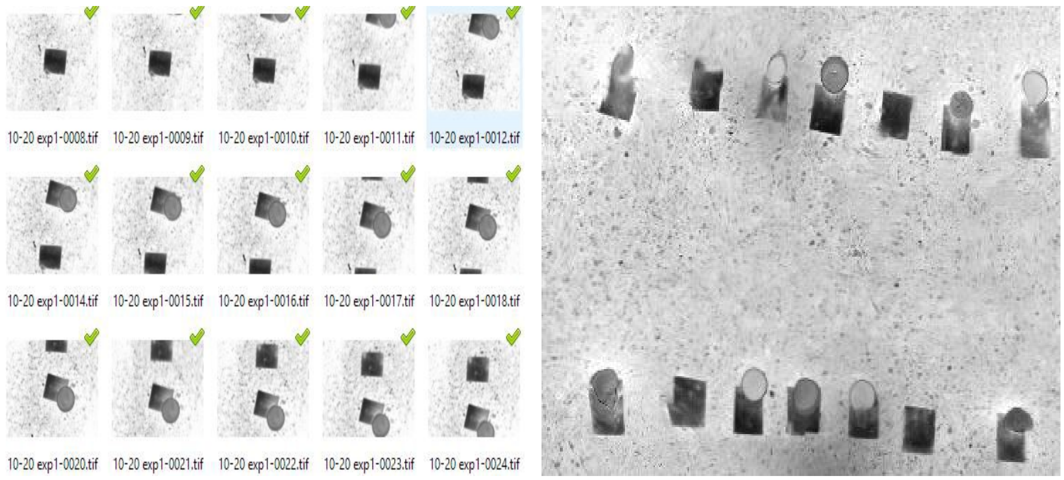

(a) Experiment field (b) Thermal picture by IR Flash

Figure 5. Stitching's effect experiment

ACKNOWLEDGMENTS

Thanks go to Mr. Yuquan Chen and Ms. Yang Zhao for helping set up the experiments and collect data. This work is supported in part by CITRIS (Center for Information Technology Research In The Interest of Society).

REFERENCES

[1] Berni, J. A., Zarco-Tejada, P. J., Suárez, L., and Fereres, E., "Thermal and narrowband multispectral remote sensing for vegetation monitoring from an unmanned aerial vehicle," *IEEE Transactions on Geoscience and Remote Sensing* **47**(3), 722–738 (2009).

[2] Gade, R. and Moeslund, T. B., "Thermal cameras and applications: a survey," *Machine Vision and Applications* **25**(1), 245–262 (2014).

[3] Martinelli, F., Scalenghe, R., Davino, S., Panno, S., Scuderi, G., Ruisi, P., Villa, P., Stroppiana, D., Boschetti, M., Goulart, L. R., et al., "Advanced methods of plant disease detection. a review," *Agronomy for Sustainable Development* **35**(1), 1–25 (2015).

[4] Zhao, T., Stark, B., Chen, Y., Ray, A., and Doll, D., "More reliable crop water stress quantification using small unmanned aerial systems (suas)," *IFAC-PapersOnLine* **49**(16), 409–414 (2016).

[5] Zhao, T., Stark, B., Chen, Y., Ray, A. L., and Doll, D., "A detailed field study of direct correlations between ground truth crop water stress and normalized difference vegetation index (NDVI) from small unmanned aerial system (sUAS)," in [*2015 International Conference on Unmanned Aircraft Systems*], 520–525 (2015).

[6] Soliman, A., Heck, R. J., Brenning, A., Brown, R., and Miller, S., "Remote sensing of soil moisture in vineyards using airborne and ground-based thermal inertia data," *Remote Sensing* **5**(8), 3729–3748 (2013).

[7] Zhao, T., Stark, B., Chen, Y., Ray, A. L., and Doll, D., "Challenges in water stress quantification using small unmanned aerial system (suas): Lessons from a growing season of almond," *Journal of Intelligent & Robotic Systems* **88**(2-4), 721–735 (2017).

[8] Zhao, T., Chen, Y., Ray, A., and Doll, D., "Quantifying almond water stress using unmanned aerial vehicles (uavs): correlation of stem water potential and higher order moments of non-normalized canopy distribution," in [*ASME 2017 International Design Engineering Technical Conferences and Computers and Information in Engineering Conference*], (2017).

[9] Zhao, T., Doll, D., Wang, D., and Chen, Y., "A new framework for UAV-based remote sensing data processing and its application in almond water stress quantification," in [*2017 International Conference on Unmanned Aircraft Systems*], 1794–1799 (2017).

[10] Sheng, H., Chao, H., Coopmans, C., Han, J., McKee, M., and Chen, Y., "Low-cost UAV-based thermal infrared remote sensing: Platform, calibration and applications," in [*2010 IEEE/ASME International Conference on Mechatronics and Embedded Systems and Applications*], 38–43 (2010).

[11] Ribeiro-Gomes, K., Hernández-López, D., Ortega, J. F., Ballesteros, R., Poblete, T., and Moreno, M. A., "Uncooled thermal camera calibration and optimization of the photogrammetry process for UAV applications in agriculture," *Sensors* **17**(10), 2173 (2017).

[12] Jones, H. G., Serraj, R., Loveys, B. R., Xiong, L., Wheaton, A., and Price, A. H., "Thermal infrared imaging of crop canopies for the remote diagnosis and quantification of plant responses to water stress in the field," *Functional Plant Biology* **36**(11), 978–989 (2009).

[13] Gowen, A., Tiwari, B., Cullen, P., McDonnell, K., and O'Donnell, C., "Applications of thermal imaging in food quality and safety assessment," *Trends in Food Science & Technology* **21**(4), 190–200 (2010).

[14] Jensen, A. M., McKee, M., and Chen, Y., "Procedures for processing thermal images using low-cost microbolometer cameras for small unmanned aerial systems," in [*IEEE International Geoscience and Remote Sensing Symposium*], 2629–2632 (2014).

[15] Bishop, C. M., [*Neural networks for pattern recognition*], Oxford university press (1995).

[16] Wallis, K. F., "Seasonal adjustment and relations between variables," *Journal of the American Statistical Association* **69**(345), 18–31 (1974).

[17] Burckle, R. A. and WinSystems, V., "PC/104 embedded modules: The new systems components," (2003).

[18] Berni, J., Zarco-Tejada, P., Suárez, L., González-Dugo, V., and Fereres, E., "Remote sensing of vegetation from UAV platforms using lightweight multispectral and thermal imaging sensors," *The International Archives of the Photogrammetry, Remote Sensing and Spatial Information Sciences* **38**(6) (2009).

[19] Wood, R. A., "Uncooled thermal imaging with monolithic silicon focal planes," in [*1993 International Symposium on Optics, Imaging, and Instrumentation*], **2020**, 322–330 (1993).

[20] Zhao, T., Doll, D., and Chen, Y., "Better almond water stress monitoring using fractional-order moments of non-normalized difference vegetation index," in [*2017 ASABE Annual International Meeting*], American Society of Agricultural and Biological Engineers (2017).